Dielectric Relaxation in Carbosilane Dendrimers with Perfluorinated End Groups

B. Trahasch and B. Stühn*

Fakultät für Physik, Hermann-Herder-Strasse 3, D-79104 Freiburg, Germany

H. Frey and K. Lorenz

Institut für Makromolekulare Chemie and Freiburger Materialforschungszentrum, Stefan-Meier-Strasse 21/31, D-79104 Freiburg, Germany

Received July 9, 1998; Revised Manuscript Received December 14, 1998

ABSTRACT: A series of carbosilane dendrimer generations G*x*RF6 ($x = 1, 2, 3$) with perfluorohexyl ($-C_6F_{13}$) end groups as well as an unmodified G3 with allyl end groups has been investigated using dielectric spectroscopy. The experiments comprised a frequency range from 2 Hz to 1 GHz. The dendrimers show a fast (β) relaxation with an Arrhenius type temperature dependence and an activation energy of 17 kJ/mol. The dominant α-process is found in all G*x*RF6 dendrimers and is split into a slow and a fast part. Its temperature dependence is the same for generation 1 and 2. At elevated T both components apparently merge. Microscopically they are related to the existence of dipole components parallel and perpendicular to the long axis in the end group. The nematic field splits the relaxational dynamics into two components. For G1RF6 a transition from a smectic to a nematic state is observed at $T = -15$ °C. It is observed in the dielectric relaxation as a discontinuous increase of the relaxation times for both components of the α-process.

I. Introduction

Dendrimers as a novel type of macromolecular architecture open new perspectives in the research in macromolecular chemistry and physics. Dendrimers are distinguished by their well-defined, highly branched structure: emanating from a central point with functionality *f*, linear segments of uniform length are attached. The end of each block represents a new branching point. The addition of each branching layer completes a generation. In this nomenclature $g = 0$ consists only of the functional center and *f* arms. Synthesis is possible via divergent and convergent routes.[1−4]

We investigated a series of carbosilane dendrimers with perfluorohexyl end groups ($-C_6F_{13}$). Synthesis and characterization of these molecules has been reported in a recent publication.[5] The molecules consist of a highly flexible carbosilane core with silicon atoms as the branching points. The perfluorinated end groups may be considered to be stiff rods. Due to the highly branched structure, crystallization of the dendrimer core is impeded.

As a result of the effective repulsive interaction between the end groups and the dendrimer core, both parts of the molecule microphase separate and form ordered domains. This superstructure depends strongly on generation and varies from a lamellar phase for generation 1 to a columnar structure for generation 3.[5] Despite their microphase-separated structure, the samples only show one glass transition temperature, which exhibits a weak dependence on generation. In the case of G1RF6 a phase transition is observed in DSC at $T_{sn} = 258$ K. Below T_{sn} the end groups are ordered in smectic layers.

The dynamics of these dendrimers on microscopic length and time scale has been studied using quasielastic neutron scattering (QUENS).[6] The advantage of this method is its resolution with respect to both space and time. In this work it was possible to separate the dynamics of the core and shell segments. The end groups were found to be locally ordered in layers. They are able to rotate along their long axis with a rotational diffusion coefficient comparable to that found in the crystalline phase of perfluorinated alkanes.[7] Segments in the dendrimer core display a diffusion behavior with a crossover from a local relaxation process to translational diffusion at small scattering vectors. The translational diffusion coefficient was found to decrease markedly with generation as opposed to the rotational diffusion coefficient which was nearly the same for all generations.

Due to the limited spectral range of the neutron scattering technique it is not possible to follow the dynamics in a wide range of temperature. We therefore turn to a different experimental method which allows to study relaxation processes in a frequency range of 1 Hz to 1GHz. In comparison to the QENS experiments, however, dielectric spectroscopy investigations observe relaxations on a longer time scale. The method provides no spatial resolution. In the present study we will present measurements of the temperature and frequency dependence of the dielectric loss in dendrimers. These investigations yield information on the dynamics of polar groups (and consequently on their molecular motions). For the carbosilane dendrimers with perfluorohexyl end groups, we observe a relaxation process which will be shown to be related to the glass transition process and a weak relaxation at lower temperatures.

II. Experimental Section

A series of carbosilane dendrimer generations G1RF6, G2RF6 to G3RF6 with perfluorohexyl ($-C_6F_{13}$) end groups have been synthesized using divergent techniques. The number of end groups varies strongly with generation (Table 1). Details of their synthesis are described elsewhere.[5] In addition we used a nonfunctionalized dendrimer of generation 3 (G3) and a linear sample M shown in Figure 1, which represents a model for the end groups without a dendritic core.

* To whom correspondence should be addressed.

10.1021/ma981075e CCC: $18.00
Published on Web 03/05/1999

Table 1. Description of the Dendrimers Used in This Study

	T_g/K	n_e	M/g
G1RF6	243	12	5364.6
G2RF6	234	36	16345.4
G3RF6	232	108	49170.7
G3	188		8112.7

[a] n_e: number of end groups. *M*: calculated molecular weight.

$$CH_3-(CH_2)_5-S-(CH_2)_2-C_6F_{13}$$

Figure 1. Sample M representing a model for the end groups without a dendrimer core.

The phase behavior of the dendrimers has been studied using DSC and X-ray scattering.[5] All dendrimers show glass transitions decreasing with generation. The glass transition temperatures T_g and the molecular weights are given in Table 1. Only G1RF6 forms a smectic mesophase between 243 and 258 K. In contrast to the dendrimers no glass transition step was observed for sample M in the DSC curve. This material is crystalline with a melting peak at $T_m = 248$ K in the heating curve. The enthalpy is $\Delta H = 49$ J/g, which is comparable to that of the perfluorinated alkane ($T_m(C_6F_{14}) = 193$ K; $\Delta H = 38$ J/g).

The dielectric measurements were performed with two different experimental setups in order to cover a wide frequency range: (I) Measurements in the frequency range from 2 Hz to 300 kHz were carried out with a Schlumberger 1260 impedance analyzer. This setup was described previously.[8] (II) For high frequency in the range between 1 and 1000 MHz we used a Hewlett-Packard impedance analyzer HP-4191-A, which is based on the principle of a reflectometer. Measuring the reflectivity of a capacitor for an electromagnetic wave enables the determination of the complex impedance of the sample. The capacitor used consists of two gold covered plates, separated by a 50 μm glass fiber spacer (to define a fixed sample thickness). The capacitor filled with the sample was assembled as a part of the waveguide of the reflectometer. This arrangement was placed in a cryostat. By use of a temperature-controlled nitrogen gas jet temperature variation between 170 and 470 K is possible. Temperature stability was better than 0.5 K. The sample temperature was directly measured at the capacitor using a platinum resistor.

The sample thickness in these measurements was only determined with a relatively large error due to the large viscosity of the samples. This error does not affect the frequency dependence of ϵ^* but only its absolute value.

III. Results and Discussion

A. Characteristics of the Dielectric Loss Spectra. Figure 2 displays the experimental result of the temperature and frequency dependence of the dielectric loss $\epsilon''(\nu)$ for the example of sample G2RF6. The results from both frequency regions have been combined. The overall form of $\epsilon''(\omega)$ observed in the figure is representative for all dendrimers G*x*RF6 ($x = 1, 2, 3$). The main features of the spectra are observed in the figure. At high temperature a relaxation process with a high dielectric loss is discernible. The relaxation frequency as marked by the maximum in $\epsilon''(\nu)$ displays a strong temperature dependence. With lowering T the relaxation is shifted to smaller frequency. It will be shown to be related to the glass transition process. In the following we refer to this relaxation as the α process. Additionally at high temperature $\epsilon''(\nu)$ is found to increase at small ν due to DC conductivity. When one goes to a lower temperature, an additional relaxation process is active. This gives rise to a dielectric loss about 20 times smaller than that of the strong relaxation. Its relaxation frequency depends only weakly on T. This relaxation process is referred to as the β process.

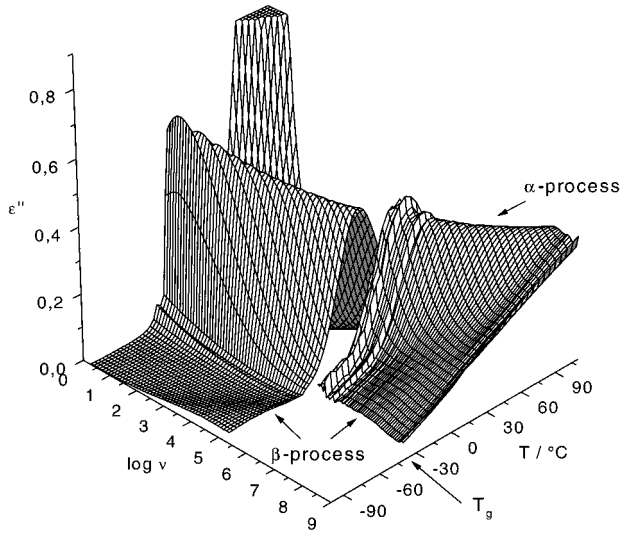

Figure 2. Three-dimensional representation of the frequency and temperature dependence of the dielectric loss for the example of G2RF6. Data from both experimental setups are combined.

To describe the spectra at a given temperature quantitatively we use a Havriliak−Negami function (HN):[9,10]

$$\epsilon^*(\nu) = \epsilon_\infty + \frac{\Delta\epsilon}{(1 + (i2\pi\nu\tau)^\alpha)^\gamma} \qquad (1)$$

where $\Delta\epsilon = \epsilon_{st} - \epsilon_\infty$ is the relaxation strength, ϵ_{st} and ϵ_∞ are the permittivities at low and high frequency, respectively. The parameter α_{HN} characterizes a symmetrical broadening, the parameter γ_{HN} an asymmetric broadening of $\epsilon''(\nu)$ if plotted on a logarithmic ν axis ($0 < \alpha_{HN}, \gamma_{HN} \leq 1$). In the case of $\alpha_{HN} = 1 = \gamma_{HN}$ the HN function reduces to a Debye relaxation process. Special cases are the Cole−Cole function ($\alpha_{HN} < 1$; $\gamma_{HN} = 1$) or the Cole−Davidson function ($\alpha_{HN} = 1$; $\gamma_{HN} < 1$).

Figure 3 displays typical dielectric loss profiles of the α process in G2RF6 and G3RF6. The curves are obviously very broad, and it was not possible to describe the data with solely one HN function. It was necessary to apply a sum of two HN functions in order to arrive at a good description of the spectra. Their superposition provides a good fit of the measured loss curve. The α process is obviously split into two spectral parts. In the following the relaxation at lower frequencies is assigned the subscript 1, α_1; the one at higher frequency is assigned as α_2. The fitted curves are included in Figure 3; the specific parameters α_{HN} and γ_{HN} are compiled in Table 2. For G2RF6 the relaxation α_2 could be described with a Cole−Cole function and fixed $\alpha_{HN} = 0.63$. For the relaxation α_1 the parameters α_{HN} and γ_{HN} vary in the range given in Table 2. With increasing temperature the value of α_{HN} increases and the value of γ_{HN} decreases. The spectrum develops an increasing width. In contrast to G2RF6 the dielectric loss curves of G3RF6 could be fitted with two Cole−Cole functions with a constant parameter α_{HN}.

We now turn to the spectrum of the first generation dendrimer G1RF6. For this sample a phase transition at $T_{sn} = 258$ K has been reported. Measurements of the texture in the polarizing microscope observe a change from a smectic S_A phase to a disordered state.[5] Its influence on $\epsilon''(\nu)$ is seen as an abrupt change of the form of the dielectric loss curve and a variation in the

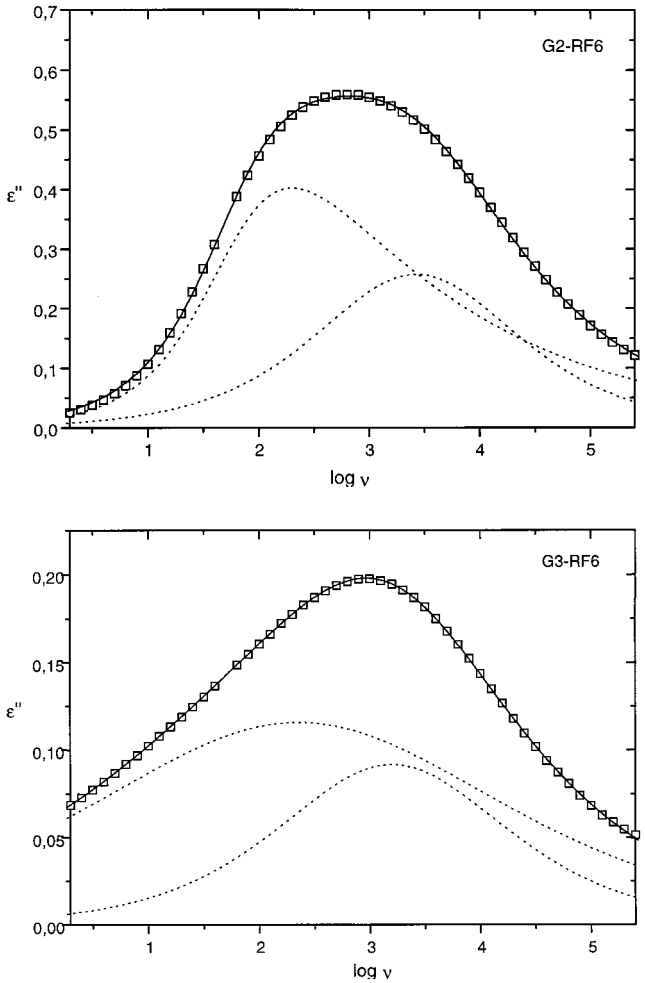

Figure 3. Frequency dependence of the dielectric loss in the α process in G2RF6 at $T = 251$ K and in G3RF6 at 248 K. The dotted lines are the components α_1 and α_2 as obtained from a fit of HN functions (eq 1). The fit is the sum of both and is shown as the full curve.

Table 2. Parameters Characterizing the Shape of $\epsilon''(\nu)$ in the Havriliak−Negami Spectrum

HN param	G1-RF6 $T > T_{sn}$	G1-RF6 $T < T_{sn}$	G2-RF6	G3-RF6	
		Low Frequency			
α_{HN}	0.95−0.96	0.97−0.99	0.85−0.99	0.34	α_1
γ_{HN}	0.32−0.35	0.33−0.35	0.20−0.33	1.00	
α_{HN}	0.68−0.77	0.53−0.68	0.63	0.57	α_2
γ_{HN}	0.76−0.95	≈1.00	1.00	1.00	
		High Frequency			
α_{HN}		0.82−0.92	0.72−0.85	≈0.64	
γ_{HN}		0.39−0.50	0.39−0.56	≈1.00	

temperature dependence of the relaxation frequencies (see Figure 4). Below and above the transition the loss spectrum is the composition of two HN functions in perfect analogy to the case of G2RF6 and G3RF6. A significant change of the broadening parameters α_{HN} and γ_{HN} above T_{sn}, especially for the relaxation α_2, is also a consequence (see Table 2): For temperatures below T_{sn} the relaxation α_2 is only symmetrically broadened. For temperatures above T_{sn} it becomes more asymmetric ($\gamma \leq 1$).

As opposed to the data in the low-frequency region, the dielectric loss curves obtained from the measurements in the high-frequency region can be described with just one HN function for all G*x*RF6. The corresponding parameters are also included in Table 2.

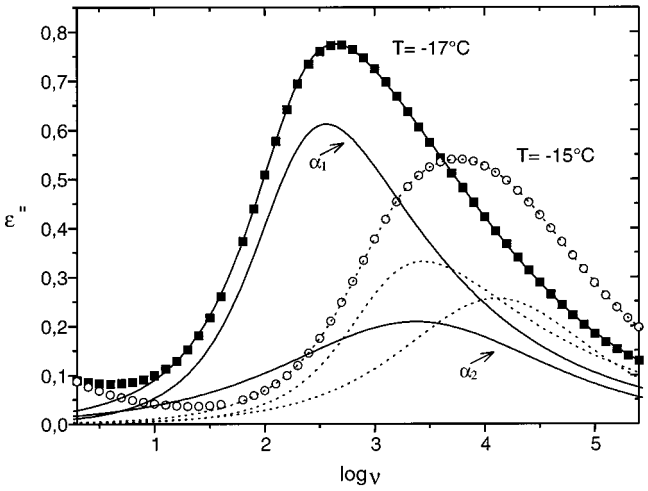

Figure 4. Frequency dependence of the dielectric loss in the α process in G1RF6 at the phase transition. The sum of the labeled curves describes the α relaxation process at $T = -17$ °C (■). The sum of the dotted curves describes the α relaxation process at $T = -15$ °C (○).

As seen in Figure 2 for G2RF6 the β relaxation at temperatures below T_g was observed in all generations of G*x*RF6 and in both frequency ranges. Due to the smaller dielectric loss, it was difficult to analyze this relaxation. Only for G2RF6 in the high-frequency region do we obtain a good description with a Cole−Cole function and a fixed parameter $\alpha_{HN} = 0.34$.

The dielectric loss spectrum of the nonfunctionalized dendrimer G3 also shows a relaxation process related to its glass transition. However, the relaxation strength of the loss curve is about factor 10 smaller than the respective relaxation strength in G3RF6. Due to the fact that the glass transition temperature of G3 is $T_g = 188$ K the measurements refer to relatively large separation form T_g and the α relaxation process may be superposed by the β relaxation process. A reliable determination of the line shape parameters was not possible and we only make use of the relaxation frequency as determined from the position of the maximum in $\epsilon''(\nu)$.

The dielectric spectrum of sample M shows a relaxation process with a strong temperature dependence and a relaxation strength in the same order of magnitude as that of G3. In addition to this, a relaxation process with a very small dielectric loss (about a factor 10 less than the dielectric loss of the strong relaxation in this sample) appears at lower temperature and at high frequency which may be compared to the β relaxation.

B. Temperature Dependence of the Relaxation Frequency. Following the description of the general features of the shape of the loss function for the dendrimers, we now proceed to a discussion of the variation of the relaxation frequencies with temperature. As was mentioned in the preceding section the functionalized dendrimers G*x*RF6 exhibit two relaxations called α and β which are characterized by their different variation with temperature.

As is seen in Figure 2 the α process is dramatically slowed when lowering temperature. This is the characteristic feature of the glass transition process. The temperature dependence of the relaxation rate ν_{max} at the maximum in $\epsilon''(\nu)$ is phenomenologically described by the Vogel−Fulcher equation:

$$\ln \nu_{max} = A - \frac{B}{T - T_v} \quad (2)$$

A, B, and T_v are the Vogel−Fulcher parameters. A represents the limiting value of the frequency for $T \rightarrow \infty$, and B describes an activation temperature. T_v is the so-called Vogel temperature, which is often found to be about 50 K below T_g. With T approaching T_v the relaxation times diverge.

In Figure 5 the α process and the β process in G2RF6 are displayed in an Arrhenius diagram. The relaxation frequency ν_{max} given in the figure is $1/\tau$ of the HN function. The errors of these data result from the fitting procedure. They are smaller than the size of the symbols and consequently not shown in the plot. The α processes in all dendrimers were found to be well described by Vogel−Fulcher functions. We were, however, not able to find a common description of the high-frequency and low-frequency domain data. This is due to the splitting of the α process observed at low temperature. In view of the limited range available for the fitting of eq 2 to the data, the Vogel temperature was fixed at $T_g - 50$ K. It is then possible to compare the results for the different dendrimers. The lines in Figure 5 represent these fits. In Table 3 the Vogel−Fulcher parameters are given for the low-frequency region; in Table 4 the parameters are presented for the high-frequency region. The difference between α_1 and α_2 is seen to be mainly the parameter A which is related to the trial frequency $\nu_0 = \exp(A)$. At high T the data extrapolate to $\nu_0 = 2.4 \times 10^{10}$ s^{-1}.

The temperature dependence of the β process can be described by an Arrhenius function (dotted line):

$$\nu_{max} \sim \exp(-E_a/RT) \quad (3)$$

The activation energy E_a is derived from the slope of the straight line in Figure 5. R is the gas constant. We obtain $E_a = 17$ kJ/mol. Here we find an extrapolated $\nu_0 = 9.7 \times 10^{10}$ s^{-1}.

For G1RF6 the phase transition at T_{si} is also discernible in the activation diagram (see Figure 6): The temperature dependence of the frequencies changes discontinuously at T_{si}. The splitting of the relaxation, however, is seen in both phases. This is reflected by the abrupt change in the fitting parameters when crossing the phase transition. On both sides of the phase transition the temperature dependence of the relaxation frequencies was well described by Vogel−Fulcher functions and fixed $T_v = 193$ K. The parameters presented in Table 3 refer to the isotropic state for all dendrimers. For temperatures $T < T_{sn}$, the parameters for relaxation α_1 increase to $A = 27.4$ and $B = 1410$ K; for relaxation α_2, the parameters decrease to $A = 18.9$ and $B = 690$ K. The change in the apparent activation energy is more clearly seen in the insert of Figure 6. The impact of the smectic isotropic phase transition on the dielectric relaxation times has also been observed in comblike liquid-crystalline polymers with perfluoroalkyl groups.[11]

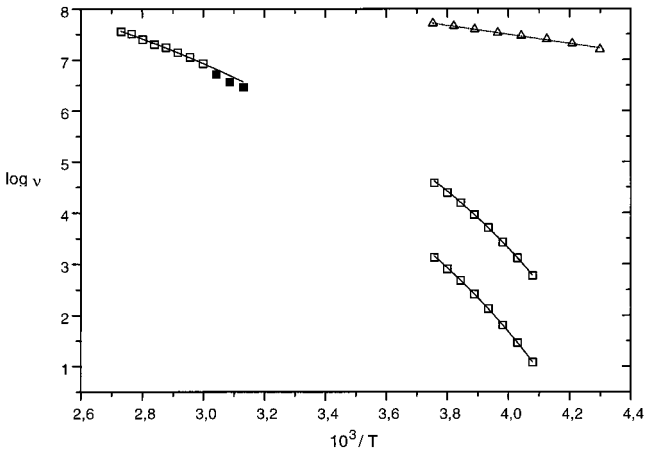

Figure 5. Temperature dependence of the relaxation processes in G2RF6 (□, α process with Vogel−Fulcher fit; △, β relaxation with Arrhenius fit). The filled squares were not used in the fit.

Table 3. Vogel−Fulcher Parameters Determined Using Eq 2 for the Glass Transition Process in the Low-Frequency Domain

	relaxation process α_1			relaxation process α_2		
	A	B/K	T_v/K	A	B/K	T_v/K
G1RF6[a]	21.4	790	193	21.6	960	193
G2RF6	21.2	1140	184	23.0	1020	184
G3RF6	23.0	1170	182	25.3	1190	182
G3	37.5	2010	135			

[a] For G1RF6 the parameters refer to $T > T_{sn}$.

Table 4. Vogel−Fulcher Parameters for the Glass Transition Process in the High-Frequency Domain

	A	B/K	T_v/K
G1RF6	24.9	1260	193
G2RF6	23.9	1210	184
G3RF6	26.2	1340	182

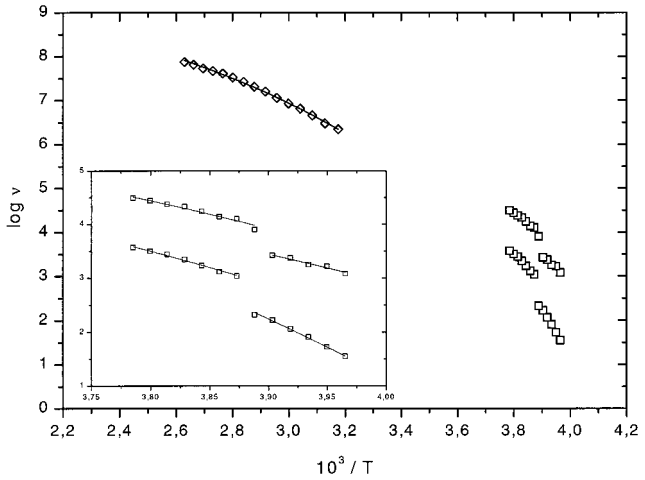

Figure 6. Temperature dependence of the α relaxation process in G1RF6 with Vogel−Fulcher fits. The inset emphasizes the range at the phase transition.

The description of the α process in G3RF6 was much more difficult. As seen in Figures 5 and 6 for G1RF6 and G2RF6, the relaxations α_1 and α_2 are parallel. This is obviously different for G3RF6. At low temperatures both relaxations appear to merge. (see Figure 7).

Finally the glass transition processes of G3RF6 and G3 and the observed relaxation in sample M are compared in Figure 7. The relaxation in G3 can be described by a Vogel−Fulcher function. The parameters, which are shown in Table 3 are much larger than the respective parameters for the functionalized dendrimer G3RF6. We emphasize the small relaxation strength in G3 as compared to G3RF6. We take this as an indication for the end groups to provide the main part of the dipole moment involved in this relaxation.

Although sample M does not show a glass transition process, the data points do not fall on a straight line in

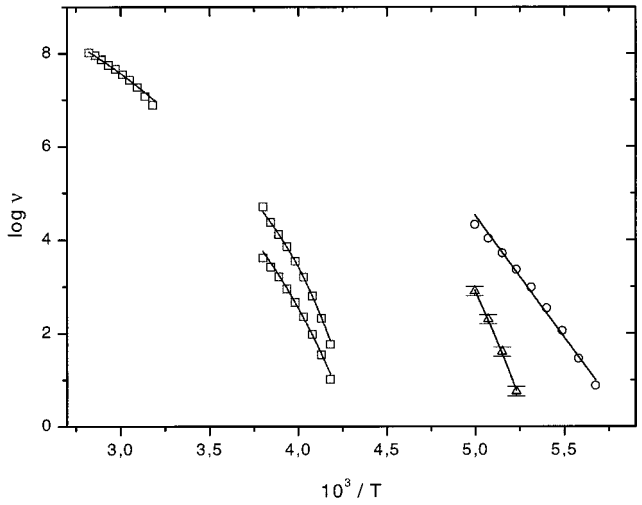

Figure 7. Comparison of the relaxation processes in G3RF6 (□), G3 (△), and sample M (○).

the Arrhenius-plot. Even below the melting point the molecules retain their rotational degree of freedom which gives rise to the observed dielectric relaxation.

IV. Conclusions

The overall features of the relaxation time spectrum of the dendrimers as observed in a dielectric spectroscopy experiment resemble that of a linear amorphous polymer. Besides a strong relaxation with a Vogel−Fulcher type temperature dependence the spectra show a side relaxation at elevated temperature which is significantly weaker in its relaxation strength. Moreover, the Vogel temperature is related to the glass transition temperature in a DSC measurement approximately as $T_g - 50$ K. On the other hand the system is found to be microphase separated and would therefore be expected to display two different glass processes referring to both domains. No second process could be detected in DSC measurements. It is therefore important to address the question of the microscopic origin of the α process and its dependence on superstructure.

A striking feature is the splitting of the relaxation time spectrum at low temperature. A similar behavior has been found in measurements on liquid crystalline side group polymers.[12−15] In these systems a separate observation of both components was possible in samples that had been macroscopically oriented in an external field. Such an orientation is not possible in our case. However, the splitting of both components is sufficiently large to enable a clear separation. On the basis of the theory of Martin, Meier, and Saupe,[16] the microscopic origin of this relaxation is found in the relaxation of the correlation of a dipole moment in parallel to the helical axis of the end groups. The splitting is the result of the nematic field acting on the molecules in order to achieve a parallel arrangement.

A prerequisite for this interpretation is the existence of a parallel component of the dipole moment in the end group. The effective dipole moment of a perfluorinated alkane such as C_6F_{14} is small as a result of the helical structure of the molecule. Although each CF bond contributes approximately $\mu_{CF} = 1.8$ D the stiff structure of the molecule leads to an effective cancellation. This scheme is modified when one of the end-standing fluorine atoms is replaced by an unpolar substituent as is the case in our dendrimers. Adding up the 12 CF bond moments along the helix one arrives at a dipole moment perpendicular to the helical axis which amounts to 16% of μ_{CF}. A second, parallel component is due to the now uncompensated end-standing fluorine and is mainly parallel to the helical axis. This simple picture is supported by an MNDO calculation using the Alchemy 2000 program. For $C_6F_{13}CH_3$ as a model substance we obtain $\mu = 3.4$ D.

As we have seen before the relaxation strength of the α relaxation process in the dendrimer G3 without end groups is about 10 times smaller than the respective relaxation strength in G3RF6. This fact supports our interpretation of the α process.

Turning to the β process of the dielectric relaxation, a microscopic origin may be seen in the relaxation of the perpendicular component of the end group dipole moment as a result of rotational diffusion. However, other molecular groups may contribute to this relaxation. The rotational diffusion of the end groups has been studied using QENS,[6] and the relaxation times observed were an order of magnitude smaller than those of the β process. The reason for this discrepancy may be seen in the selected q range of the neutron scattering experiment. In direct space it comprises distances up to 1.6 nm. Correlations that extend beyond this length are excluded but contribute to the relaxation of the dielectric function.

The variation of the dielectric relaxation with superstructure of the dendrimers is best seen in the example of G1RF6. The phase transition at T_{sn} leads to a discontinuous shift in the relaxation time of both the α_1 and the α_2 process (see Figure 6). The splitting, however, is present in both states. We take this as evidence for the persistence of orientational order in the high temperature state. The end groups are chemically fixed to the dendrimer core and are therefore unable to adopt an isotropically disordered state. This distinguishes the dendrimers from liquid crystalline side-chain polymers.

References and Notes

(1) Tomalia, D. A.; Naylor, A. M.; Goddard, A. M., III. *Angew. Chem.* **1990**, *102*, 119−157.
(2) Issberner, I.; Moors, R.; Vögtle, F. *Angew. Chem.* **1994**, *106*, 2507−2514.
(3) Tomalia, D. A.; Durst, H. D. *Top. Curr. Chem.* **1993**, *165*, 193−313.
(4) Newkome, G. R.; Moorefield, C.; Vögtle, F. *Dendritic Molecules—Concepts, Synthesis, Perspectives*; Verlag Chemie: Weinheim, Germany, New York, 1996; Frey, H.; Lach, C.; Lorenz, K. *Adv. Mater.* **1998**, *10*, 279.
(5) Lorenz, K.; Frey, H.; Stühn, B.; Mühlhaupt, R. *Macromolecules* **1997**, *30*, 6860.
(6) Stark, B.; Stühn, B.; Frey, H.; Lach, C.; Lorenz, K.; Frick, B. *Macromolecules* **1998**, *31*, 5415−5423.
(7) Kimmig, M.; Steiner, R.; Strobl, G.; Stühn, B. *J. Chem. Phys.* **1993**, *99*, 8105−8114.
(8) Stühn, B.; Stickel, F. *Macromolecules* **1992**, *25*, 5306.
(9) Havriliak, S.; Negami, S. *J. Polym. Sci., Part C* **1966**, *14*, 99.
(10) Havriliak, S.; Negami, S. *Polymer* **1967**, *8*, 161.
(11) Alig, I.; Braun, D.; Jarek, M.; Hellmann, G. P. *Macromol. Symp.* **1995**, *90*, 173−194. Alig, I.; Jarek, M.; Hellmann, G. P. *Macromolecules*, in press.
(12) Haase, W.; Pranoto, H.; Bormuth, F. J. *Ber. Bunsen-Ges. Phys. Chem.* **1985**, *89*, 1229−1234.
(13) Bormuth, F. J.; Biradar, A. M.; Quotschalla, U.; Haase, W. *Liq. Cryst.* **1989**, *5*, 1549−1557.
(14) Zhong, Z. Z.; Schuele, E. E.; Gordon, W. L. *Liq. Cryst.* **1994**, *17*, 199−209.
(15) Götz, S.; Stille, W.; Strobl, G.; Scheuermann, H. *Ber. Bunsen-Ges. Phys. Chem.* **1993**, *97*, 1315−1320.
(16) Martin, A. J.; Meier, G.; Saupe, A. *Symp. Faraday Soc.* **1971**, *5*, 119.

MA981075E